Archives of Dermatological Research (2019) 311:711–719
https://doi.org/10.1007/s00403-019-01961-6

ORIGINAL PAPER

Association between sphingosine-1-phosphate-induced signal transduction via mitogen-activated protein kinase pathways and keloid formation

Seung Hyo Jung[1] · Yu Kwan Song[2] · Hong Chung[3] · Hyun Myung Ko[4] · Sung Hoon Lee[5] · Dong In Jo[2] · Bokyung Kim[1] · Dong Hee Lee[6] · Soon Heum Kim[2]

Received: 17 December 2018 / Revised: 23 June 2019 / Accepted: 27 July 2019 / Published online: 5 August 2019

Abstract

We conducted this experimental study to analyze the relationship between sphingosine-1-phosphate (S1P)-induced mitogen-activated protein (MAP) kinase pathways and keloid formation. We collected samples of the normal tissue and the keloid tissue from 10 normal healthy individuals and 12 patients with keloid scars, respectively. Then, we compared the level of sphingosine-1-phosphate receptor (S1PR1/S1PR2) mRNA/protein expression between the normal tissue and the keloid tissue. Moreover, we also compared the level of S1PR protein expression, that of S1P-induced COL1A1 (collagen Type I, α-1 chain) expression, that of S1P-induced JNK/ERK phosphorylation, that of S1P-induced COL1A1 expression following the treatment with 30 μM PD98059 (ERK inhibitor) or 30 μM SP600125 (JNK inhibitor) and that of S1P-induced COL1A1 expression following the treatment with W146 (S1PR1 inhibitor) or JTE013 (S1PR2 inhibitor) between the normal fibroblasts and the keloid fibroblasts. We found that the level of S1PR1/S1PR2 mRNA/protein expression was significantly higher in the keloid tissue as compared with the normal tissue. Our results also showed that the level of S1P-induced COL1A1 expression and that of S1P-induced JNK/ERK phosphorylation were significantly higher in the keloid fibroblasts as compared with the normal ones ($P < 0.05$). Furthermore, there were significant decreases in the level of S1P-induced COL1A1 expression when the keloid fibroblasts were treated with 30 μM SP600125 or 30 μM PD98059 and that of S1P-induced COL1A1 expression when the treated with 100 nM W146 or 100 nM JTE013 ($P < 0.05$). Our results indicate that S1P-induced signal transduction is associated with increased collagen synthesis via S1PR-mediated signaling pathways in the keloid tissue.

Keywords Sphingosine-1-phosphate · Mitogen-activated protein kinase · Keloid scars · Fibroblasts · Signal transduction

✉ Soon Heum Kim
plastic7@kku.ac.kr

[1] Research Institute of Medical Science, Konkuk University School of Medicine, 82 Gugwon-daero, Chungju 27376, Korea

[2] Department of Plastic and Reconstructive Surgery, Konkuk University School of Medicine, Konkuk University Chungju Hospital, 82 Gugwon-daero, Chungju 27376, Korea

[3] Department of Medicine, Konkuk University School of Medicine, Konkuk University Chungju Hospital, 82 Gugwon-daero, Chungju 27376, Korea

[4] Department of Eco-Biological Science, College of Science and Technology, Woosuk University, Jincheon-eup, Jincheon-gun, Chungbuk 27841, Korea

[5] Department of Pharmacy, College of Pharmacy, Chung-Ang University, 84 Heukseok-Ro, Dongjak-Gu, Seoul 06974, Korea

[6] Gyeongbuk Institute for Bio Industry, Gyeongbuk, Korea

Introduction

Molecules and the relevant pathways have been studied at cellular levels in association with the pathophysiology of keloid. Collagen, matrix metalloproteinase-1 (MMP-1), also known as interstitial or fibroblast collagenase, and tissue inhibitors of metalloproteinases (TIMPs) suppressing the activity of MMP-1 are present in the normal dermis. These components have antagonistic effects against each other, thus playing a role in regulating the amount of collagen [4]. Arciniegas et al. showed that a variety of molecules are involved in the thickening of the dermis in association with the keloid formation; these include versican, syndecan-1, fibronectin, thrombospondin-1, tenascin C, CD44, integrin β1 and N-cadherin. These authors also confirmed the presence of galectin-1 and -3 (Gal-1 and -3)

in the cytoplasm and the cell membrane of cells involved in the keloid formation [3].

Factors associated with increased or decreased collagen synthesis are involved in the pathogenesis of keloid [9]. This leads to the speculation that therapeutics suppressing collagen synthesis and promoting collagenase expression might be useful for the treatment of keloid. Hypoxic characteristics of keloid are closely associated with actions of hypoxia-inducible factor-1α (HIF-1α) that mediates responses to hypoxic stress and thereby adapt cells to hypoxic conditions. According to Lei et al., Parkin played a role as an E3 ubiquitin ligase in mediating the degradation of HIF-1α in keloid fibroblasts. This is accompanied by findings not only that HIF-1α was up-regulated due to the silencing of Parkin in keloid fibroblast, but also that its levels were affected by Parkin via transforming growth factor β (TGF-β)/Smad signaling pathway. Thus, these authors noted that Parkin would promote the proliferation of keloid fibroblasts and then inhibit their apoptosis via TGF-β/Smad signaling pathway [20].

According to animal studies, interferon-γ (IFN-γ) suppressed the collagen synthesis and the formation of fibrous tissue [14]. It has been therefore used for the treatment of keloid [6]. Moreover, this is accompanied by a published study showing that its effects are closely associated with decreased ceramide levels [21]. It has been reported that ceramide inhibits the growth of fibroblasts and increases MMP-1 levels [31]. This indicates the applicability of ceramide to the treatment of keloid. Unlike normal fibroblasts, however, keloid ones resist ceramide-induced apoptosis through up-regulation of insulin-like growth factor-I receptor (IGF-IR) [16]. It has therefore been suggested that ceramide therapy is not effective for the treatment of keloid [15].

Both sphingosine and ceramide belong to sphingolipids. They are rich in cell membranes and play a role in mediating the signal transduction [13].

Ceramide is synthesized de novo or produced from sphingomyelin degradation. Sphingosine is produced through deacylation of ceramide. Moreover, it can also be converted to ceramide via a salvage pathway or from sphingosine-1-phosphate (S1P) through the mediation of sphingosine kinase 1 and 2 [2]. Cell growth is stimulated or inhibited with actions of ceramide, sphingosine or S1P depending on the type of cells. It is generally known that ceramide and sphingosine inhibit the cell growth and S1P promotes the cell proliferation [18, 29]. Therefore, the regulation of the inter-convertible sphingolipid metabolites, ceramide and S1P, and their opposing signaling pathways, referred to as the "sphingolipid rheostat", serves as a major indicator of cell fate [24]. Moreover, it has also been reported that tumor necrosis factor-α (TNF-α)-induced apoptosis occurs with the involvement of sphingosine generated from ceramide rather than ceramide produced from the activation of neutral sphingomyelinase [12].

S1P is a signal transducer that has emerged as a key regulator of numerous biological functions, such as the growth, differentiation, survival and apoptosis [7]. Mitogen-activated protein (MAP) kinases are involved in the regulation of cell growth, differentiation and apoptosis [23]. Moreover, they play a role in regulating actions of activator protein-1 (AP-1), and TGF-β is involved in the activation of AP-1 transcriptional factor [35]. Furthermore, their three subfamilies, such as extracellular signal-regulated kinase (ERK), p38 kinase and c-Jun N-terminal kinase (JNK), are known to play a key role in mediating the cellular response to extracellular stimuli. Thus, ERK and p38 kinase phosphorylation is involved in the differentiation of fibroblasts, whereas JNK phosphorylation plays a role in their proliferation [5, 23, 38]. Previous reports have suggested that S1P-induced signal transduction occurs via MAP kinase pathways mediated by extracellular signal-regulated kinase (ERK) and c-Jun N-terminal kinase (JNK) [28, 36].

The S1P receptors (S1PRs) are a class of G protein-coupled ones, and they are targets of S1P. They are classified into five subtypes: S1PR1, S1PR2, S1PR3, S1PR4 and S1PR5, and play a role in regulating biological functions, such as cell proliferation, angiogenesis, migration, cytoskeleton organization, endothelial cell chemotaxis, immune cell trafficking and mitogenesis. Moreover, they are also involved in immune-modulation and suppression of innate immune responses from T cells [36].

Given the above background, we conducted this experimental study to analyze the relationship between S1P-induced MAP kinase pathways and keloid formation. The current experiment consists of two parts: comparison of S1PR expression levels between the normal tissue and the keloid tissue following the collection of tissue samples from human subjects (Experiment 1) and that of S1P-induced collagen synthesis levels, S1P-induced JNK/ERK phosphorylation levels, S1P-induced collagen synthesis levels via S1P-induced JNK/ERK phosphorylation and S1P-induced collagen synthesis levels via S1PR-mediated signaling pathways between the normal fibroblasts and the keloid fibroblasts (Experiment 2).

Methods

Experimental materials

The S1P, W146 and JTE013 were purchased from Cayman Chemical (Ann Arbor, MI). McCoy's 5A medium was obtained from Welgene (Daegu, Korea). Anti-S1PR1 and -S1PR2 antibodies were obtained from the Abcam (Cambridge, UK). In addition, anti-CO1LA1, -p-JNK and -t-JNK

antibodies and PD98059 were obtained from the Cell Signaling Technology (Boston, MA). Furthermore, anti-GAPDH, -P-ERK and -T-ERK antibodies were purchased from Santa Cruz Biotechnology (Santa Cruz, CA). SP600125 was purchased from Sigma-Aldrich (St. Louis, MO).

Normal and keloid fibroblasts were purchased from the American Type Culture Collection (Rockville, MD) and then cultured in Dulbecco's Modified Eagle's Medium (DMEM) containing 10% fetal bovine serum (FBS), 100 U/mL penicillin, 100 µg/mL streptomycin and 200 mM glutamine. The cells were used at passages 5–8, grown to 70–80% confluence and starved in DMEM without FBS for 12 h.

Experiment 1

The Experiment was performed to compare levels of S1PR mRNA/protein expression, for which we collected tissue samples from 12 patients with keloid scar (4 men and 8 women; mean age = 37.3 ± 12.7 years; mean disease duration = 2.9 ± 3.3 years) and 10 normal healthy individuals (4 men and 6 women; mean age = 40.4 ± 11.7 years). Thus, normal and keloid tissue samples (0.1–0.2 mg each) were obtained from the peripheral area of the skin lesion. Sites of tissue sampling include earlobe (5 cases), chest (3 cases), abdomen (1 case), shoulder (1 case), forearm (1 case) and posterior neck (1 case) in the patients with keloids and eyelid (6 cases), breast (2 cases), forearm (1 case) and back (1 case) in normal controls.

For the Experiment 1, we included men or women aged 18 years or older, the patients with a diagnosis of keloids defined as the protrusion of the excessive scar tissue above the skin level or its proliferation beyond the margin of the original lesion and those who had no past history of taking any treatments for keloid scars. But we excluded women who are pregnant or breastfeeding, the patients with underlying diseases (e.g., diabetes mellitus, hepatic diseases or renal insufficiency), those with open wounds at the site of or near the lesion, those with infectious lesion and those who were deemed to be ineligible for study participation according to our judgment. We evaluated their baseline and clinical characteristics through a retrospective review of the medical records.

The tissue samples were rinsed in a saline (136.9 mM NaCl, 5.4 mM KCl, 1.5 mM $CaCl_2$, 1.0 mM $MgCl_2$, 23.8 mM $NaHCO_3$ [pH 7.5] and 0.01 mM ethylenediaminetetraacetic acid [EDTA]). They were snap frozen in liquid nitrogen for further laboratory procedures. The tissue samples were immersed in 4% paraform aldehyde for 8 h and then prepared into a formalin-fixed, paraffin-embedded block. Thus, a total of 22 tissue blocks were finally obtained and then sectioned at a thickness of 10 µm for immunohistochemistry (IHC).

Tissue sections were treated with blocking serum at room temperature for 1 h to inhibit non-specific binding. They were incubated with a 1:100 dilution of anti-S1PR1 and -S1PR2 antibodies overnight at 4 °C. After being washed with phosphate buffered saline (PBS) for 10 min, they were incubated with a 1:200 dilution of biotinylated secondary antibody at room temperature for 1 h. This was followed by a 30-min incubation of the sections with horseradish peroxidase-conjugated dextran polymer reagent kits (ChemMate Envision Kit K5007; DakoCytomation, Glostrup, Denmark). The peroxidase activity was visualized with 3,3′-diaminobenzidine tetrachloride according to the manufacturer's instructions. The sections were counterstained with hematoxylin at room temperature. Negative controls were carried out by omitting the primary antibodies. This was followed by semi-quantitative assessment of nuclear and cytoplasmic expressions of anti-S1PR1 and -S1PR2 antibodies in three categories: (1) diffuse strong (> 50%) (2) weak or focal (< 50%) and (3) no staining. The sections were stained with 3,3′-diaminobenzidine (DAB) and then examined using the BX51 light microscope (Olympus, Tokyo, Japan). Quantification of the IHC intensity was performed using ImageJ software.

RNA was extracted with laser captured microdissection using TRIzol Reagent (Invitrogen, Carlsbad, CA) according to the manufacturer's instructions. Total RNA (1 µg) was reverse transcribed into cDNA using the SuperScript™ III First-Strand Synthesis System (Invitrogen). Real-time polymerase chain reaction (RT-PCR) was performed using the iQ™ SYBR Green Supermix and iCycler iQ Real-Time PCR Detection System (Bio-Rad Laboratories, Hercules, CA). All the samples were amplified in triplicate in a 96-well plate in the following conditions: 3 min at 95 °C and 40 cycles at 95 °C for 10 s followed by 30 s at 60 °C. The relative mRNA expression level was determined by calculating the value of the Δcycle threshold (ΔCt), for which the average Ct value was normalized by its endogenous control glyceraldehyde-3-phosphate dehydrogenase (GAPDH) and $2^{-\Delta\Delta Ct}$ was calculated [22]. To do this, the values were expressed as fold-change in the keloid group from the control group. The RT-PCR was performed using the following primer sets: S1PR1 (NP_001307659.1) forward, 5′-TGCTCTCCATCG TCATTCTG-3′, reverse, 5′-CCAGGAAGTACTCCGCTC TG-3′; S1PR2 (NP_004221.3) forward, 5′-CCAAGCATT ATGTGCTGTGC-3′, reverse, 5′-CAGAAGGAGGATGCT GAAGG -3′; and GAPDH (P04406) forward, 5′-TGATGG GTGTGAACCACGAG-3′, reverse, 5′-GGGCCATCCACA GTCTTCTG-3'.

For western blotting, the samples were prepared into lysates. This was followed by the centrifugation at 16,000*g* for 15 min at 4 °C. Protein concentrations in the supernatant were determined using Bio-Rad DC protein assay reagents (Bio-Rad Laboratories), which was followed by the dilution

using the SDS sample buffer containing 40 mM Tris–HCl (pH 6.8), 8 mM EGTA, 4% 2-mercaptoethanol, 40% glycerol, 0.01% bromophenol blue and 4% sodium dodecyl sulfate (SDS) and a 10-min boiling. But western blotting of CO1LA1 was performed in a non-reducing condition. An equivalent number of samples were prepared and then mounted on 12% SDS–polyacrylamide gel electrophoresis (PAGE) and then transferred electrophoretically to polyvinylidene difluoride (PVDF). The membrane was blocked with PBS containing 5% fat-free dried milk and then incubated overnight at 4 °C, with each antibody diluted at a ratio of 1:1000–5000. Thus, immune complexes were incubated for 1 h with a peroxidase-conjugated antibody diluted at a ratio of 1:5000. This was followed by the application of the secondary antibody. Then, the blots were incubated in enhanced chemiluminescence kits (Amersham Pharmacia, Piscataway, NJ). Band intensity was quantified using the Luminescent Image Analyzer LAS-3000 (Fujifilm, Tokyo, Japan).

Experiment 2

In the Experiment 2, normal fibroblasts were treated with S1P, S1P + W146 or S1P + JTE013, but those not treated with S1P served as controls. Similarly, keloid fibroblasts were treated with S1P, S1P + W146 or S1P + JTE013, but those not treated with S1P served as controls. This was followed by analysis of the level of S1P-induced (collagen Type I, α-1 chain) COL1A1 expression in both normal and keloid fibroblasts.

Levels of CO1LA1 expression were assessed using the standard immunostaining method. Briefly, the fibroblasts were fixed with 10% formaldehyde at room temperature for 1 h for the purposes of inhibiting non-specific binding. After being washed twice with PBS containing 0.05% Tween 20 and then permeabilized with 0.1% Triton X-100 in PBS for 5 min, they were incubated with primary antibodies against COL1A1, diluted at a ratio of 1:500, for overnight at 4 °C. Thus, immune complexes were incubated with Alexa-488-conjugated secondary antibody diluted at a ratio of 1:1000 for 1 h. This was followed by examination using fluorescence microscopy (Axio Observer A, Zeiss, Jena, Germany). Then, the RT-PCR and western blotting were performed.

Statistical analysis

All data was expressed as mean ± SEM (SEM: standard error of the mean). Values are compared using the one-way analysis of variance (ANOVA) or Student's *t* test, followed by a post hoc analysis using the Dunnett test. A *P* value of < 0.05 was considered statistically significant.

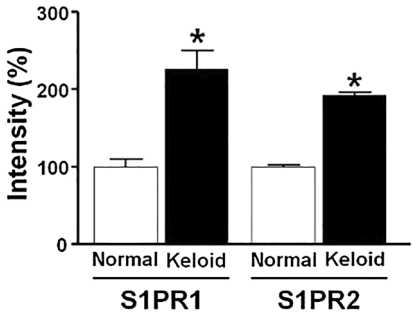

Fig. 1 Immunohistochemical findings of and the intensity of immunohistochemistry of the keloid tissue and the normal one. The percentage of positive immunohistochemical findings of each tissue section was approximately 1.5-fold higher in the keloid tissue as compared with the normal one, which reached statistical significance ($P < 0.05$). *Statistical significance at $P < 0.05$

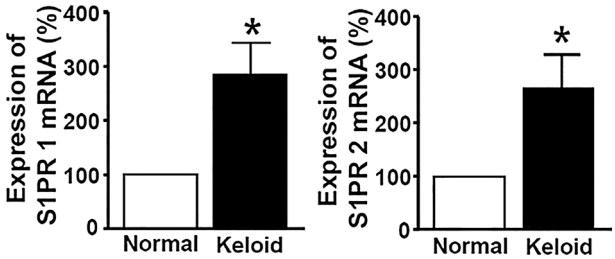

Fig. 2 Levels of S1PR1/S1PR2 mRNA expressions. The level of S1PR mRNA expression was about 1.5-fold significantly higher in the keloid tissue as compared with the normal tissue. This difference reached statistical significance ($P < 0.05$). *Statistical significance at $P < 0.05$

Results

Results of the Experiment 1

We compared the level of S1PR (S1PR1/S1PR2) expression between the normal tissue and the keloid tissue. On IHC, the percentage of positive IHC findings was significantly higher in the keloid tissue as compared with the normal one (Fig. 1).

The level of S1PR1/S1PR2 mRNA expression was about 1.5-fold significantly higher in the keloid tissue as compared with the normal one ($P < 0.05$) (Fig. 2). Moreover, the level of S1PR1/S1PR2 protein expression was significantly higher in the keloid tissue as compared with the normal one ($P < 0.05$) (Fig. 3).

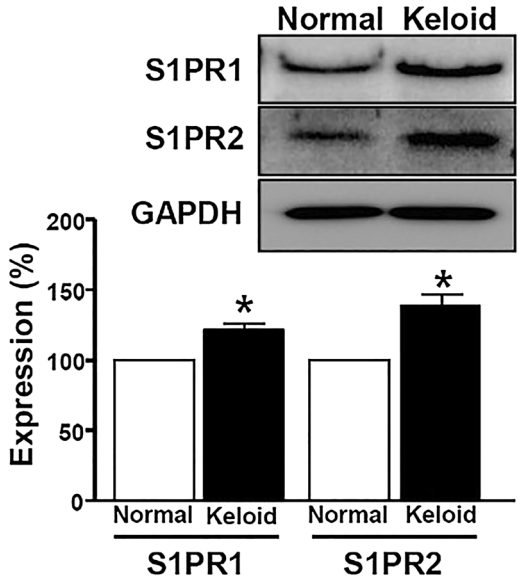

Fig. 3 Levels of S1PR1/S1PR2 protein expressions. The level of S1PR1/S1PR2 protein expression was significantly higher in the keloid tissue as compared with the normal one ($P<0.05$). GAPDH served as a loading control. *Statistical significance at $P<0.05$

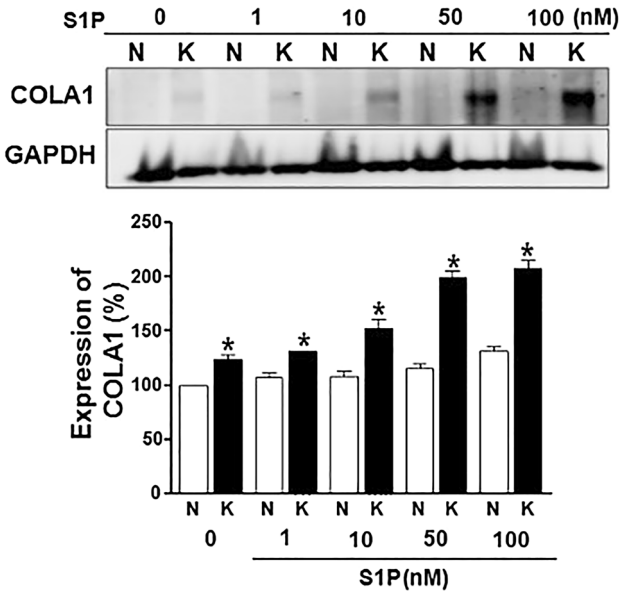

Fig. 4 The level of S1P-induced COL1A1 expression. The level of S1P-induced COL1A1 expression was significantly higher in the keloid fibroblasts as compared with the normal ones ($P<0.05$). Moreover, it reached the maximum when the keloid fibroblasts were treated with 100 nM S1P for 24 h ($n=3$; Fig. 4). GAPDH served as a loading control. N, normal fibroblasts; K, keloid fibroblasts; COL1A1, collagen type 1 gene. *Statistical significance at $P<0.05$

Results of the Experiment 2

To examine whether S1P is involved in the collagen synthesis, we compared the level of S1P-induced COL1A1 expression between the keloid fibroblasts and the normal ones. The level of S1P-induced COL1A1 expression was significantly higher in the keloid fibroblasts as compared with the normal ones ($P<0.05$) (Fig. 4). Thus, it reached the maximum when the keloid fibroblasts were treated with S1P 100 nM for 24 h ($n=3$; Fig. 4).

We examined whether there is a significant difference in the level of S1P-induced JNK/ERK phosphorylation between the keloid fibroblasts and normal ones. The level of S1P-induced JNK/ERK phosphorylation was significantly higher in the keloid fibroblasts as compared with the normal ones ($P<0.05$) (Fig. 5a). Thus, it reached the maximum when the keloid fibroblasts were treated with S1P 100 nM for 30 min (Fig. 5b). Moreover, there was a dose-dependent increase in the level of S1P-induced JNK/ERK phosphorylation within a range of S1P dose (0–100 nM); it reached the maximum at a dose of 50 nM. But the level of GAPDH expression had no significant correlation with S1P treatment.

To examine whether the level of S1P-induced COL1A1 expression is associated with that of S1P-induced JNK/ERK phosphorylation, we treated the keloid fibroblasts with 30 μM SP600125 (JNK inhibitor) or 30 μM PD98059 (ERK inhibitor). The level of S1P-induced COL1A1 expression reached the maximum (100 nM) in the keloid fibroblasts at 24 h. But it was inhibited when the keloid fibroblasts were treated with 30 μM SP600125 or 30 μM PD98059. Moreover, there was a significant decrease in the level of S1P-induced COL1A1 expression at 24 h after the keloid fibroblasts were treated with 30 μM SP600125 or 30 μM PD98059 ($P<0.05$) ($n=6$; Fig. 6).

To examine whether the level of S1P-induced COL1A1 expression is associated with S1PR-mediated signaling pathways, we treated the keloid fibroblasts with 100 nM W146 (S1PR1 inhibitor) or 100 nM JTE013 (S1PR2 inhibitor). There was a significant decrease in the level of S1P-induced COL1A1 expression when the keloid fibroblasts were treated with 100 nM W146 or 100 nM JTE013 ($P<0.05$) (Fig. 7).

Discussion

To date, cellular and molecular pathophysiology of keloid scars have been studied, but little is understood about them. The keloidogenesis arises from multiple factors; these include wound tension, skin pigmentation, genetic predisposition, immunoregulation and skin injury [11, 39].

In the current study, there was a dose-dependent increase in the level of S1P-induced COL1A1 expression. In addition, it was significantly higher in the keloid fibroblasts as compared with the normal ones. These results strongly indicate that S1P is associated with increased collagen synthesis and fibrosis, thus contributing to the formation of keloid scars.

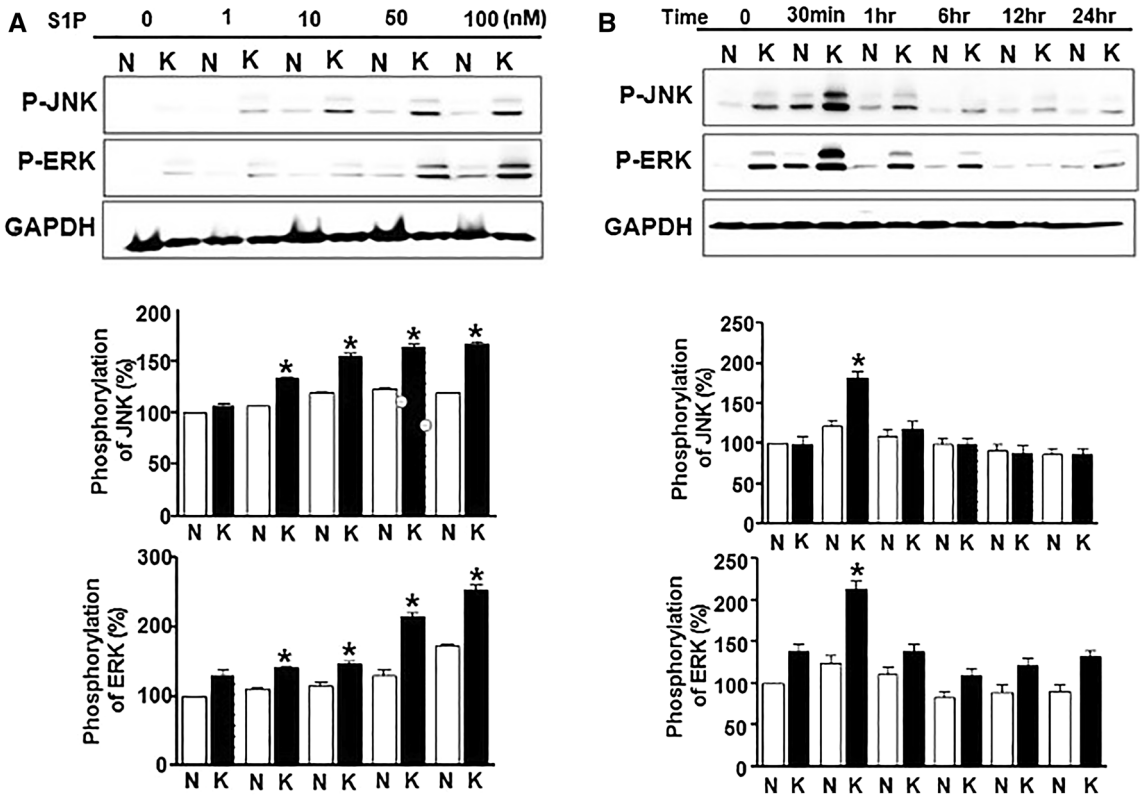

Fig. 5 The level of S1P-induced JNK/ERK phosphorylation. The keloid fibroblasts and the normal ones were treated with S1P at varying concentrations (0–100 nM) for 30 min (**a**) and for the indicated times (**b**). **a** The cell lysates were immunoblotted with anti-JNK, -ERK and -GAPDH antibodies. The lower panels show statistical results obtained from the upper ones. The response of the cells was considered 100% under quiescent conditions. The level of S1P-induced JNK/ERK phosphorylation of was significantly higher in the keloid fibroblasts as compared with the normal ones ($P<0.05$). **b** After the treatment with 100 nM S1P for 30 min, it reached the maximum. GAPDH served as a loading control. N, normal fibroblasts; K, keloid fibroblasts. *Statistical significance at $P<0.05$

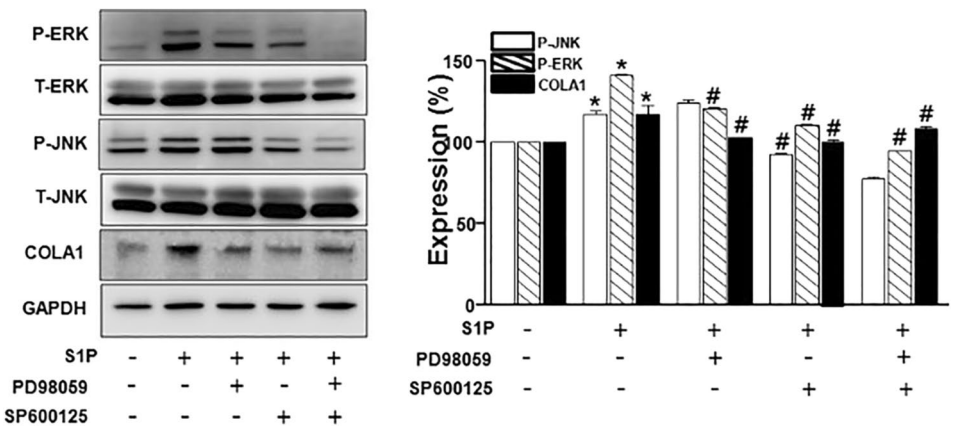

Fig. 6 The level of S1P-induced COL1A1 expression via S1P-induced JNK/ERK phosphorylation. The level of COL1A1 expression reached the maximum (100 nM) in the keloid fibroblasts at 24 h. But it was inhibited when the keloid fibroblasts were treated with 30 μM SP600125 or 30 μM PD98059. Moreover, there was a significant decrease in the level of S1P-induced COL1A1 expression at 24 h after the keloid fibroblasts were treated with 30 μM SP600125 or 30 μM PD98059 ($P<0.05$) ($n=6$; Fig. 6). COL1A1, collagen type 1 gene. *Statistical significance at $P<0.05$ vs. S1P-untreated cells; $^{\#}P<0.05$ vs. S1P-treated cells

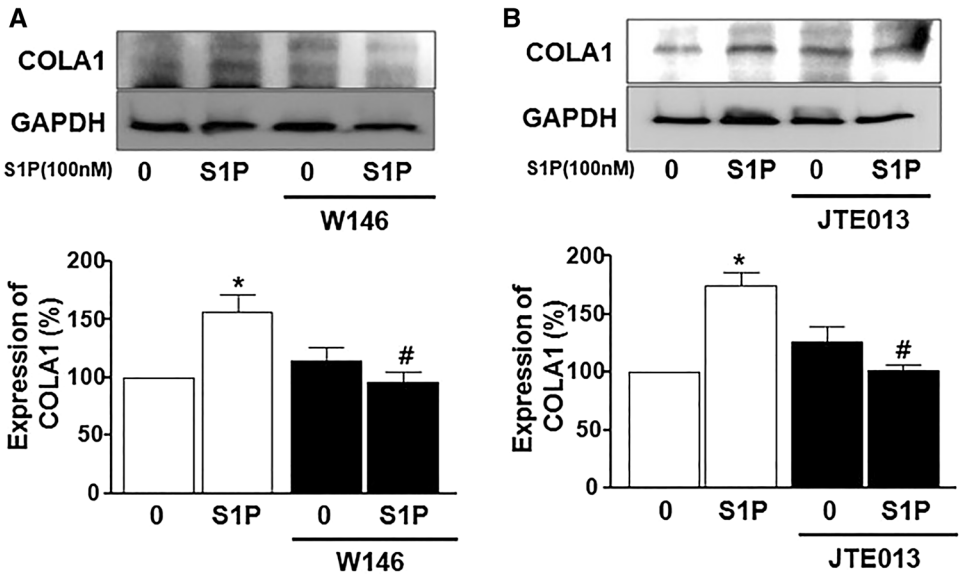

Fig. 7 The level of S1P-induced COL1A1 expression via S1PR-mediated signaling pathways. There was a significant decrease in the level of S1P-induced COL1A1 expression when the keloid fibroblasts were treated with 100 nM W146 (**a**) or 100 nM JTE013 (**b**) ($P < 0.05$). DIC, differential interference contrast; COL1A1, collagen type 1 gene. *Statistical significance at $P < 0.05$ vs. S1P-untreated cells; $^{\#}P < 0.05$ vs. S1P-treated cells

This is in agreement with a previous published study showing that keloid scars are characterized by increased collagen deposition, resulting in tissue hypertrophy, and angiogenesis [1].

We found that the level of S1P-induced COL1A1 expression was significantly higher in the keloid fibroblasts as compared with the normal ones, which is also consistent with a prior publication [30]. In our previous experiment, analyzing the status of collagen deposition and S1PRs in biopsy samples obtained from patients with keloid scars, we showed that the keloid tissue had an abundant presence of collagen on immunofluorescence, an increase in the number of S1PRs in the keloid tissue sample and a twofold higher level of S1P-induced COL1A1 expression in the keloid fibroblasts as compared with the normal ones on the RT-PCR and western blotting [17].

After comparing the level of S1PR1/S1PR2 expression between the experimental groups, we found that it was significantly higher in the keloid fibroblasts as compared with the normal ones. It can therefore be inferred that S1P is a biomarker associated with increased collagen synthesis [10].

Our results also showed that there was a significant positive correlation between the level of S1P-induced COL1A1 expression and that of S1PR1/S1PR2 expression [33]. In addition, we also found that there was a dose-dependent increase in the level of S1P-induced JNK/ERK phosphorylation [25]. Additionally, our results also showed that ERK and JNK antagonists and S1PR1/S1PR2 inhibitors reduced the level of S1P-induced COL1A1 expression [34]. These results indicate that MAP kinases and sphingolipid, particularly including S1P, are closely associated with collagen synthesis in the keloid tissue. The S1P-induced signal transduction via MAP kinase pathways plays a role in regulating the differentiation and proliferation of keloid fibroblasts [19]. It can therefore be inferred that alterations in it through the regulation of JNK/ERK phosphorylation are closely associated with those in S1P-induced COL1A1 expression in the keloid tissue such as hypertrophic scars. Moreover, there was a significant decrease in the level of S1P-induced COL1A1 expression when the keloid fibroblasts were treated with W146 and JTE013 [37]. These results indicate that it is regulated by S1P-induced signal transduction involved in MAP kinase pathways in the keloid tissue.

MAP kinases also have positive or negative effects on apoptosis of fibroblasts; p38 kinase and JNK play a role in inducing the apoptosis but ERK inhibits it. This is consistent with a report showing that the keloid tissue was characterized by down-regulation of apoptosis-related genes as compared with the normal one [27]. Therefore, induction of apoptosis in keloid fibroblasts might be another treatment strategy for patients with keloid scars.

In the current study, we found that the level of S1PR1/S1PR2 expression, that of S1P-induced COL1A1 expression and that of S1P-induced JNK/ERK phosphorylation were significantly higher in the keloid fibroblasts as compared with the normal ones ($P < 0.05$). Moreover, our results also showed that there were significant decreases in the level of S1P-induced COL1A1 expression when the keloid fibroblasts were treated with 30 μM SP600125 or 30 μM PD98059 and that of S1P-induced COL1A1 expression when the treated with 100 nM W146 or 100 nM JTE013 ($P < 0.05$). But our results cannot be generalized because we failed to analyze the effects of S1P on the proliferation of normal and keloid fibroblasts. This deserves further studies.

The management of keloid scars poses a challenge for clinicians. To date, single treatment modality or its combination with other regimens have been attempted to treat it. It remains problematic, however, that none of these treatments

are a treatment of choice and their efficacy, if any, may be limited because of adverse events [26, 33]. As described in the current results, increased collagen synthesis is closely associated with the pathophysiology of keloid scars. Efforts have therefore been made to inhibit the collagen synthesis; these include intralesional corticosteroid injections, cryotherapy, pressure therapy, radiotherapy, laser therapy, the use of onion extract, topical application of imiquimod cream, belomycin, IFN and photodynamic therapy [8].

Conclusions

In conclusion, our results indicate that S1P-induced signal transduction is associated with increased collagen synthesis via S1PR-mediated signaling pathways in the keloid tissue. It can therefore be inferred that modifications in regulators involved in S1P-induced signal transduction via MAP kinase pathways might be useful in treating keloid scars. But this deserves further clinical studies.

Acknowledgments This work was supported by the Korean Research Foundation grant funded by the Korean Government (KRF-2010–0006841).

Funding Non-applicable.

Compliance with ethical standards

Conflict of interest The authors declared that they have no conflict of interest.

Informed consent Informed consent of the patients was waived due to retrospective nature of the current study. But their normal controls submitted a written informed consent.

Ethical standards The current study was conducted in accordance with the Declaration of Helsinki. The experimental protocol was approved by the Institutional Review Board (IRB) of our medical institution (IRB approval # CR316049). All the experimental procedures were performed during September of 2016.

References

1. Al-Attar A, Mess S, Thomassen JM, Kauffman CL, Davison SP (2006) Keloid pathogenesis and treatment. Plast Reconstr Surg 117:286–300
2. An D, Na C, Bielawski J, Hannun YA, Kasper DL (2011) Membrane sphingolipids as essential molecular signals for Bacteroides survival in the intestine. Proc Natl Acad Sci USA 108(Suppl 1):4666–4671
3. Arciniegas E, Carrillo LM, Rojas H, Ramírez R, Chopite M (2019) Galectin-1 and galectin-3 and their potential binding partners in the dermal thickening of keloid tissues. Am J Dermatopathol 41:193–204
4. Brew K, Nagase H (2016) The tissue inhibitors of metalloproteinases (TIMPs): an ancient family with structural and functional diversity. Biochim Biophys Acta 1803:55–71
5. Chang NS (2000) TGF-beta-induced matrix proteins inhibit p42/44 MAPK and JNK activation and suppress TNF-mediated IkappaBalpha degradation and NF-kappaB nuclear translocation in L929 fibroblasts. Biochem Biophys Res Commun 267:194–200
6. Dohi T, Miyake K, Aoki M et al (2015) Tissue inhibitor of metalloproteinase-2 suppresses collagen synthesis in cultured keloid fibroblasts. Plast Reconstr Surg Glob Open 3:e520
7. Gamard CJ, Dbaibo GS, Liu B, Obeid LM, Hannun YA (1997) Selective involvement of ceramide in cytokine-induced apoptosis. Ceramide inhibits phorbol ester activation of nuclear factor kappaB. J Biol Chem 272:16474–16481
8. Gauglitz GG (2013) Management of keloids and hypertrophic scars: current and emerging options. Clin Cosmet Investig Dermatol 6:103–114
9. Gill SE, Parks WC (2008) Metalloproteinases and their inhibitors: regulators of wound healing. Int J Biochem Cell Biol 40:1334–1347
10. Hait NC, Maiti A (2017) The role of sphingosine-1-phosphate and ceramide-1-phosphate in inflammation and cancer. Mediators Inflamm 2017:4806541
11. He S, Liu X, Yang Y et al (2010) Mechanisms of transforming growth factor beta(1)/Smad signalling mediated by mitogen-activated protein kinase pathways in keloid fibroblasts. Br J Dermatol 162:538–546
12. Heffernan-Stroud LA, Obeid LM (2013) Sphingosine kinase 1 in cancer. Adv Cancer Res 117:201–235
13. Hu ZC, Tang B, Guo D et al (2014) Expression of insulin-like growth factor-1 receptor in keloid and hypertrophic scar. Clin Exp Dermatol 39:822–828
14. Huang C, Murphy GF, Akaishi S, Ogawa R (2013) Keloids and hypertrophic scars: update and future directions. Plast Reconstr Surg Glob Open 1:e25
15. Ishihara H, Yoshimoto H, Fujioka M et al (2000) Keloid fibroblasts resist ceramide-induced apoptosis by overexpression of insulin-like growth factor I receptor. J Invest Dermatol 115:1065–1071
16. Kim S, Kim Y, Lee Y, Chung JH (2008) Ceramide accelerates ultraviolet-induced MMP-1 expression through JAK1/STAT-1 pathway in cultured human dermal fibroblasts. J Lipid Res 49:2571–2581
17. Kim SH, Jung SH, Chung H et al (2014) Annexin A2 participates in human skin keloid formation by inhibiting fibroblast proliferation. Arch Dermatol Res 306:347–357
18. Kitatani K, Idkowiak-Baldys J, Hannun YA (2008) The sphingolipid salvage pathway in ceramide metabolism and signaling. Cell Signal 20:1010–1018
19. Kye KC, Chae EK, Piao YJ et al (2004) Signaling events during induction of plasminogen activator inhibitor-1 expression by sphingosylphosphorylcholine in cultured human dermal fibroblasts. J Invest Dermatol 122:1365–1371
20. Lei R, Shen J, Zhang S et al (2019) Inactivating the ubiquitin ligase Parkin suppresses cell proliferation and induces apoptosis in human keloids. J Cell Physiol. https://doi.org/10.1002/jcp.28332
21. Lee JH, Kim SE, Lee AY (2008) Effects of interferon-alpha2b on keloid treatment with triamcinolone acetonide intralesional injection. Int J Dermatol 47:183–186
22. Livak KJ, Schmittgen TD (2001) Analysis of relative gene expression data using real-time quantitative PCR and the 2(-Delta Delta C(T)) Method. Methods 25:402–408
23. Maceyka M, Payne SG, Milstien S, Spiegel S (2002) Sphingosine kinase, sphingosine-1-phosphate, and apoptosis. Biochim Biophys Acta 1585:193–201

24. Ponnusamy S, Meyers-Needham M, Senkal CE et al (2010) Sphingolipids and cancer: ceramide and sphingosine-1-phosphate in the regulation of cell death and drug resistance. Future Oncol 6:1603–1624
25. Ryu JM, Baek YB, Shin MS et al (2014) Sphingosine-1-phosphate-induced Flk-1 transactivation stimulates mouse embryonic stem cell proliferation through S1P1/S1P3-dependent β-arrestin/c-Src pathways. Stem Cell Res 12:69–85
26. Saray Y, Güleç AT (2005) Treatment of keloids and hypertrophic scars with dermojet injections of bleomycin: a preliminary study. Int J Dermatol 44:777–784
27. Sayah DN, Soo C, Shaw WW et al (1999) Downregulation of apoptosis-related genes in keloid tissues. J Surg Res 87:209–216
28. Spiegel S, Merrill AH Jr (1996) Sphingolipid metabolism and cell growth regulation. FASEB J 10:1388–1397
29. Strub GM, Maceyka M, Hait NC, Milstien S, Spiegel S (2010) Extracellular and intracellular actions of sphingosine-1-phosphate. Adv Exp Med Biol 688:141–155
30. Syed F, Ahmadi E, Iqbal SA, Singh S, McGrouther DA, Bayat A (2011) Fibroblasts from the growing margin of keloid scars produce higher levels of collagen I and III compared with intralesional and extralesional sites: clinical implications for lesional site-directed therapy. Br J Dermatol 164:83–96
31. Tawada C, Kanoh H, Nakamura M et al (2014) Interferon-γ decreases ceramides with long-chain fatty acids: possible involvement in atopic dermatitis and psoriasis. J Invest Dermatol 134:712–718
32. van den Broek LJ, Limandjaja GC, Niessen FB, Gibbs S (2014) Human hypertrophic and keloid scar models: principles, limitations and future challenges from a tissue engineering perspective. Exp Dermatol 23:382–386
33. Wang XQ, Liu YK, Qing C, Lu SL (2009) A review of the effectiveness of antimitotic drug injections for hypertrophic scars and keloids. Ann Plast Surg 63:688–692
34. Watters RJ, Wang HG, Sung SS, Loughran TP, Liu X (2011) Targeting sphingosine-1-phosphate receptors in cancer. Anticancer Agents Med Chem 11:810–817
35. Whitmarsh AJ (2007) Regulation of gene transcription by mitogen-activated protein kinase signaling pathways. Biochim Biophys Acta 1773:1285–1298
36. Wu J, Spiegel S, Sturgill TW (1995) Sphingosine 1-phosphate rapidly activates the mitogen-activated protein kinase pathway by a G protein-dependent mechanism. J Biol Chem 270:11484–11488
37. Xiu L, Chang N, Yang L et al (2015) Intracellular sphingosine 1-phosphate contributes to collagen expression of hepatic myofibroblasts in human liver fibrosis independent of its receptors. Am J Pathol 185:387–398
38. Yeap YY, Ng IH, Badrian B et al (2010) c-Jun N-terminal kinase/c-Jun inhibits fibroblast proliferation by negatively regulating the levels of stathmin/oncoprotein 18. Biochem J 430:345–354
39. Zhang GY, Gao WY, Li X et al (2009) Effect of camptothecin on collagen synthesis in fibroblasts from patients with keloid. Ann Plast Surg 63:94–99